

JOURNAL OF ADVANCED APPLIED SCIENCES

e-ISSN: 2979-9759



RESEARCH ARTICLE

The Production of Rice Husk Ash and Blast Furnace Slag-Based Alkali-Activated Composites under High-Temperature Effects

Ahmet Filazi[™] • Nesrin Kurtoğlu • Fatih Kural •

Kırıkkale University, Kırıkkale Vocational School, Department of Construction Technology, Kırıkkale/Türkiye

ARTICLE INFO

Article History

Received: 01.12.2024 Accepted: 17.12.2024 First Published: 30.12.2024

Keywords

Alkali-activated slag concrete Blast furnace slag Fire resistance Rice husk ash



ABSTRACT

Alkali-activated concretes offer several advantages over conventional Portland cement-based concretes, including environmental sustainability, cost-effectiveness, and improved permeability. The use of alkali-activated concretes, as a replacement for Portland cement, provides significant environmental benefits, such as reducing carbon dioxide emissions by up to 80%, and facilitates the recycling and reuse of industrial and agricultural by-products. This study focuses on the development of alkali-activated concrete by incorporating industrial by-products like blast furnace slag and rice husk ash. A mixture of alkali-activated concrete based on blast furnace slag will be prepared, with partial substitution of Portland cement by these by-products by weight. The study will investigate the effects of these substitutions on the flexural and compressive strengths of the concrete over periods of 7, 28, and 90 days, as well as its fire resistance at temperatures of 200, 400, 600, and 800°C. The aim of this research is to contribute to the advancement of alkali-activated concrete technology, promoting the use of industrial by-products in the creation of more sustainable and environmentally-friendly construction materials.

Please cite this paper as follows:

Filazi, A., Kurtoğlu, N., & Kural, F. (2024). The production of rice husk ash and blast furnace slag-based alkali-activated composites under high-temperature effects. *Journal of Advanced Applied Sciences*, *3*(2), 66-78. https://doi.org/10.61326/jaasci.v3i2.318

1. Introduction

The growing demand for cement, coupled with its significant greenhouse gas emissions and the high expenses associated with Portland cement (PC), has driven efforts to explore alternative, sustainable materials. Cement manufacturing accounts for approximately 5-7% of worldwide carbon dioxide emissions, highlighting the environmental impact of traditional production processes (Colangelo et al., 2021; Mathew & Joseph, 2018). Pozzolanic materials like fly ash, blast furnace slag, and silica fume are increasingly used to minimize Portland cement consumption, driving significant

research interest in cement-free alternatives (Mehta & Siddique, 2018).

Alkali-activated composites (AAS), derived from industrial by-products like slag, fly ash, and rice husk ash, form sustainable geopolymer concretes. These materials react with alkaline activators to create a strong alumina-silicate network, with high-temperature curing enhancing strength. Their use reduces energy consumption and greenhouse gas emissions (Zhan et al., 2018). Alkali-activated concrete (AAS) offers a sustainable alternative to traditional cement by reducing carbon emissions and utilizing low-cost industrial by-products, addressing disposal issues. Heat-cured geopolymer concrete

[™] Correspondence

E-mail address: ahmetfilazi@kku.edu.tr



performs similarly or better than conventional concrete (Hardjito & Rangan, 2005; Sarker et al., 2013), but ambient curing needs further research. Heat-cured AAS can reduce CO2 emissions by up to 80% (Singh & Middendorf, 2020). Geopolymers are innovative and sustainable building materials that serve as an eco-friendly alternative to traditional concrete binders. They are synthesized through the reaction of siliconand aluminum-rich materials with alkaline activators, resulting in a durable, high-performance matrix. Commonly utilized raw materials for geopolymers include industrial by-products such as fly ash, metakaolin, and blast furnace slag, which not only reduce environmental waste but also minimize the carbon footprint of construction. A particularly noteworthy combination involves blast furnace slag and rice husk ash, which together form a robust geopolymer concrete. This mixture leverages the high reactivity of slag and the silica content of rice husk ash, producing a material with superior mechanical properties and resistance to chemical attack. By incorporating these readily available and often discarded materials, geopolymer technology aligns with principles of resource efficiency and circular economy, paving the way for more sustainable infrastructure development (Amran et al., 2021; Arularasi et al., 2021; Habert et al., 2011).

Hossain et al. (2021) found that incorporating 10-20% rice husk ash (RHA) by weight enhanced both short-term and long-term geopolymer properties. Similarly, Hwang and Huynh (2015) observed a 97% increase in tensile strength after 56 days of curing at 10 M NaOH, when 35% RHA was added to fly ash-based geopolymers. One-part geopolymers synthesized from rice husk ash (RHA) and sodium aluminate achieved a compressive strength of approximately 30 MPa, significantly higher than comparable materials, due to the almost complete reaction of RHA and the absence of crystalline byproducts (Sturm et al., 2016). Kim et al. (2014) used 10 M NaOH and sodium silicate to activate RHA in geopolymer mortar, achieving a compressive strength of 45 MPa after 28 days, demonstrating good resistance to sulfate and acid. The strength increased with higher alkali concentration and RHA content.

Manzoor et al. (2024) emphasize the potential of geopolymer concrete as a sustainable and fire-resistant alternative to traditional concrete, capable of enduring temperatures up to 1200°C while mitigating environmental impacts through the use of alumina- and silica-rich waste materials. study focuses on the use of blast furnace slag and rice husk ash, industrial by-products, to create alkali-activated concrete. The impact of replacing blast furnace slag with RHA (at 0%, 5%, 10%, 15%, 20%, and 25% by weight) on fire resistance and strength properties at various temperatures (200°C, 400°C, 600°C, 800°C) is explored.

2. Materials and Methods

2.1. Materials

The materials used in this study include Blast Furnace Slag (BFS), Rice Husk Ash (PK), and various activators. BFS, an industrial by-product, will serve as one of the primary components in the production of alkali-activated composite mortar. It is obtained by grinding the slag formed during the iron metallurgy processes in blast furnaces. The chemical composition of BFS shows low amounts of Al₂O₃, Fe₂O₃, and SO₃, but high levels of CaO, indicating a dominant calcium content compared to other compounds. Rice Husk Ash (PK) will be used as a partial replacement for BFS by weight. PK is primarily composed of SiO₂, indicating that it is silica-based, with higher potassium oxide (K₂O) content compared to sodium oxide (Na₂O), suggesting a higher presence of potassium ions (Table 1).

The activators used in this study include Sodium Hydroxide (NaOH), which will initiate and accelerate the alkali-activation process, and Sodium Silicate (Na₂SiO₃), which will be used to influence the reaction rate and improve the mechanical properties of the mortar. The sodium silicate solution used has a chemical composition of SiO₂ (26.5%), Na₂O (8.3%), and dH₂O (6.2%). Additionally, CEN Standard Sand, sourced from the Limak Batı Çimento San. ve Tic. A.Ş. Trakya Cement Factory, will be used to determine the mechanical properties of the mortar. The grain size distribution of the reference sand complies with the standards set by the European Standards Committee (CEN). These materials will be utilized to produce alkali-activated composite mortars, and their mechanical properties will be analyzed, contributing to the development of sustainable construction materials and the effective use of industrial by-products.

Table 1. Composition and characteristics of blast furnace slag and rice husk ash.

Oxides (%)	BFS	RHA
SiO ₂	35.22	89.95
Al_2O_3	17.53	2.86
Fe_2O_3	0.67	1.92
CaO	37.62	0.83
MgO	5.52	0.62
SO_3	0.68	0.46
Na ₂ O	0.42	0.18
K_2O	1.73	3.09
Density (g/cm ³)	2.89	1.97
Blaine fineness (cm ² /g)	3955	5750
Loss on Ignition (%)	1.84	7.3

2.2. Composite Mortar Production

The details of the experiments conducted to optimize the production process and strength properties of alkali-activated slag (AAS) are provided below (Table 1). For the silica source in AAS, BFS and PK were ground to cement fineness and used as binders. Standard sand was chosen as the aggregate. Sodium hydroxide (NaOH) was used in varying amounts as the activator. The alkali-activated composite samples were cast into molds of 50x50x50 mm dimensions, according to ASTM C109 standards (ASTM International, 2002), and poured using NaOH alkali solution. Sodium hydroxide was dissolved in tap

water in the laboratory to prepare the caustic solution, and the activation solution was allowed to cool to room temperature before casting the samples. The samples were cured in an oven at different temperatures and durations, for example, in the range of 70, 90, and 110°C for 24 hours. Additionally, some samples were prepared and directly subjected to thermal curing. Strength tests were conducted to determine the optimal curing time, solution molarity ratio, water-to-binder ratio, and curing temperature. Detailed information, including material quantities and sample naming, is provided in the tables. This study primarily focuses on determining the optimal curing time and optimal curing temperature.

Table 2. Mixing ratios for AAS mortars.

Mixture Name	RHA (%)	BFS (%)	Molarity (NaOH)	Curing Temperature	Curing Time	Fiber Ratio	Fire resistance (°C)
P0Y100	0	100					
P10Y90	5	95	10M 12M 14M	M 90°C	24 hours	Non- Fibrous Fibrous	200
P20Y80	10	90					400 600
P30Y70	15	85					
P40Y60	20	80		110 C			800
P50Y50	25	75					
Total Parameters	6		3	3	1	2	4

2.3. Test Procedures

2.3.1. Compression and flexural testing

The AAS (alkali-activated slag) mortar mixtures were subjected to rigorous testing to evaluate their compressive and flexural strengths in accordance with TS EN 196-1 standards. For the compressive strength assessment, six 40×40×40 mm cement mortar specimens were prepared and tested using a hydraulic compression machine. The load was applied at a rate of (2400±200) N/s to ensure consistency and precision in the testing process. After the flexural strength determination, the fractured mortar prisms were carefully positioned between the compression testing plates, ensuring proper alignment to avoid

any misalignment or skewing during the testing procedure. The compression test continued until the specimens fractured under the applied load.

To calculate the compressive strength of the mortar mixtures, the average result from the six specimens was taken, excluding any data points that deviated more than $\pm 10\%$ from the overall average. This exclusion criterion was employed to maintain the reliability and accuracy of the results. By following this procedure, a comprehensive evaluation of the compressive and flexural strength properties of the AAS mortar mixtures was achieved, providing valuable insight into the performance of the material under different loading conditions.



Figure 1. Compressive strength test.

2.3.2. Water absorption of AAS composite mortars

The water absorption characteristics of AAS composite mortar samples, with dimensions of $50\times50\times50$ mm, were assessed for 28-day specimens following ASTM C642 standards (ASTM International, 2006) (Figure 2). The mortar samples were cured in a water tank with potable water for a specified period. After curing, the specimens were removed, dried using a towel, and weighed in a saturated surface-dry condition (B). Subsequently, the samples were placed in an oven at $110\pm5^{\circ}$ C for 24 hours. After cooling to room temperature (20°C to 25°C), the samples were re-weighed (A). The water absorption rate was calculated using the formula [(B - A) / A] × 100.



Figure 2. Archimedes balance.

2.3.3. Chloride permeability of AAS composite mortars

AAS (alkali-activated slag) composite mortar specimens, which had been cured for 7 and 28 days, were tested for chloride ion permeability using the Rapid Chloride Permeability Test (RCPT) as per ASTM C1202 standards (ASTM International, 2012). These specimens were prepared by casting the mortar into Ø100×50 mm cylindrical molds (Figure 3), allowing for consistent and uniform specimen dimensions throughout the testing process. The chloride permeability test is designed to evaluate the ability of the mortar to resist the penetration of chloride ions, which is a key indicator of the material's durability, especially in environments exposed to de-icing salts or marine conditions. In this test, a voltage is applied across the specimen, and the rate at which chloride ions penetrate the material is measured. For the test, after the curing period, the specimens were subjected to the specified conditioning procedures as outlined in the ASTM C1202 standard. This typically involves placing the specimens in a testing apparatus where a voltage is applied across the specimen, with one side exposed to a chloride solution and the other side exposed to distilled water. The electrical current passed through the specimen is then measured, and the total charge passed during the test is calculated. The chloride ion permeability is evaluated based on the total charge passed through the specimen, expressed in coulombs. This value provides a direct assessment of the material's resistance to chloride penetration, where lower values indicate better resistance to chloride ion ingress, suggesting higher durability and suitability for use in environments prone to chloride exposure. By conducting this test on the AAS composite mortar specimens after 7 and 28 days of curing, the study aimed to assess the development of chloride permeability over time and the potential of the AAS mortars to perform well in terms of long-term durability.



Figure 3. Chlorine permeability of AAS composite mortars.

2.3.4. Ultrasonic transit time test

AAS composite mortar samples, with dimensions of $40\times40\times160$ mm, were tested using an ultrasonic transit time method to assess their internal properties. Sound waves at a frequency of 55 kHz were transmitted through the samples

using an ultrasonic device with a sensitivity of $0.1~\mu s$. The transit times of the sound waves were measured according to ASTM C597 standards (ASTM International, 2003). These measurements were used to calculate the sound transit velocity, providing insights into the material's density and internal

structure. Based on the measured transit times (t, μ s), the sound transit velocity (Vs, km/s) was calculated (Table 3).

Table 3. Practical evaluation of ultrasound transmission speeds.

Speed (km/s)	≥4.5	3.5-4.5	3.0-3.5	2.0-3.0	≤2.0	
Concrete quality	Very Good	Good	Medium	Poor	Very Poor	

2.3.5. High temperature experiment

The geopolymer mortar specimens, which had been cured for 28 days, were prepared for high-temperature testing to evaluate their thermal stability and performance under extreme conditions. For consistency, three replicate samples were taken from each batch of specimens. The high-temperature experiments were conducted using a high-temperature furnace, ensuring precise control over the heating process. The furnace was programmed to increase the temperature at a controlled rate of 5°C per minute, allowing for uniform heating and minimizing thermal shock to the specimens (Figure 4). During the test, each geopolymer mortar specimen was exposed to a series of target temperatures: 200°C, 400°C, 600°C, and 800°C. These temperatures were maintained for a period of one hour to simulate prolonged exposure to elevated temperatures. The specimens were carefully monitored to ensure that the desired temperature was consistently maintained throughout the exposure period. This step was crucial in assessing how the mortar would behave when subjected to varying degrees of heat, which could affect its mechanical properties, such as strength and stability. After the one-hour exposure to each target temperature, the furnace was turned off, and the specimens were allowed to cool gradually within the furnace.

The cooling process was controlled to prevent any rapid temperature changes that could induce cracking or other forms of thermal damage to the mortar samples. The specimens were left to cool to ambient temperature naturally, without forced air circulation, to allow for a more uniform cooling rate and to observe any potential changes in the material properties as it returned to room temperature (Figure 5).



Figure 4. High temperature furnace.



Figure 5. a) Room temperature b) 200°C c) 400°C d) 600°C compressive strength after sample image.

The condition of the specimens subjected to compressive testing at room temperature is shown in Figure 5. These specimens were examined through compressive tests conducted after exposure to temperatures of 200°C, 400°C, and 600°C. Beyond 800°C, it was observed that the specimens completely disintegrated at this stage. This highlights the significant impact of high temperatures on the specimens, particularly the pronounced loss of structural integrity at temperatures reaching 800°C.

3. Results and Discussion

This study aimed to evaluate the fire resistance of mixtures containing rice husk ash and BFS under different molarities and curing temperatures. The results obtained are as follows.

3.1. Molarity and Fire Resistance

Figure 6 presents the data showing the compressive strength values at varying molarities and temperatures. The study explores five molarity levels (8M, 10M, 12M, 14M) across three different temperatures (70°C, 90°C, 110°C). The findings

highlight a consistent trend: an increase in molarity results in higher compressive strength. Additionally, elevated temperatures generally contribute to improved compressive strength, with the most notable enhancement seen at 110°C.

The maximum compressive strength is achieved at a molarity of 12M and a temperature of 110°C. All tests were performed using a 12M sodium hydroxide solution, with curing carried out at 110°C.

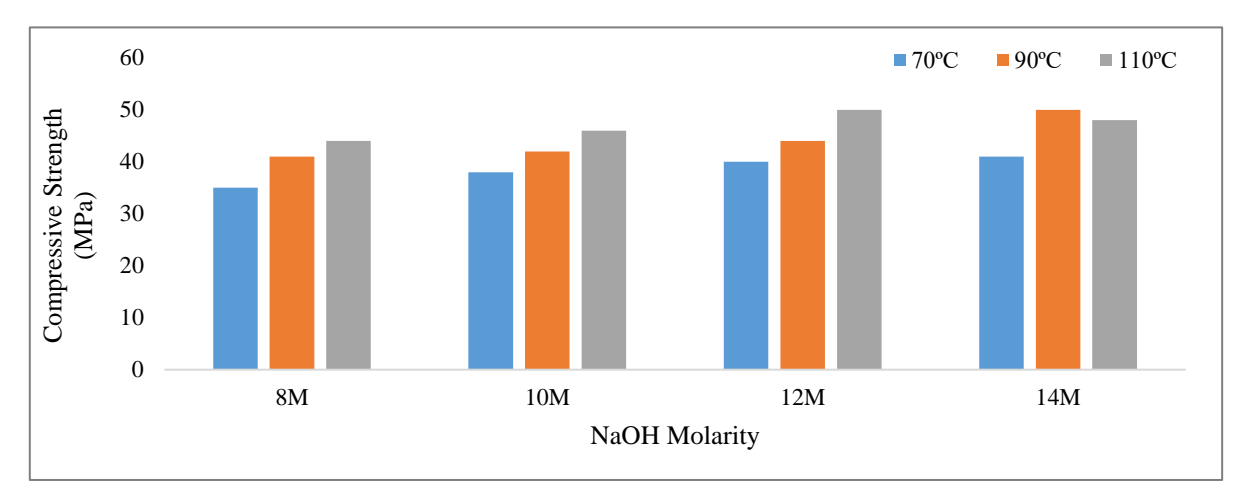


Figure 6. Compressive strength at different molarities and temperatures.

Similar findings are observed in the literature. Memon et al. (2013) reported that increasing the sodium hydroxide molarity from 8M to 14M enhanced compressive strength, with the highest strength achieved at 12M molarity and 70°C curing temperature. Mathew and Isaac (2020) demonstrated a 63% increase in compressive strength for laterized geopolymer concrete as NaOH molarity was increased. Moreover, Adam and Horianto (2014) found that curing at 120°C yielded the highest compressive strength compared to lower temperatures.

At specific temperatures, compressive strength generally increases with molarity. This finding confirms that sodium hydroxide molarity is a critical factor affecting fire resistance. Additionally, high compressive strength values observed at

110°C highlight the positive impact of elevated curing temperatures.

Curing with 12M molarity and 110°C provides the highest compressive strength. This suggests that a specific combination of molarity and temperature is most effective. All experiments were conducted using 12M sodium hydroxide molarity and cured at 110°C, emphasizing that the results are valid under these conditions. These findings clearly demonstrate how sodium hydroxide molarity and curing temperature influence compressive strength.

3.2. Compressive Strength

The results of 3, 7, 28 and 90-day compressive strength tests of AAS composite mortars are shown in Figure 7.

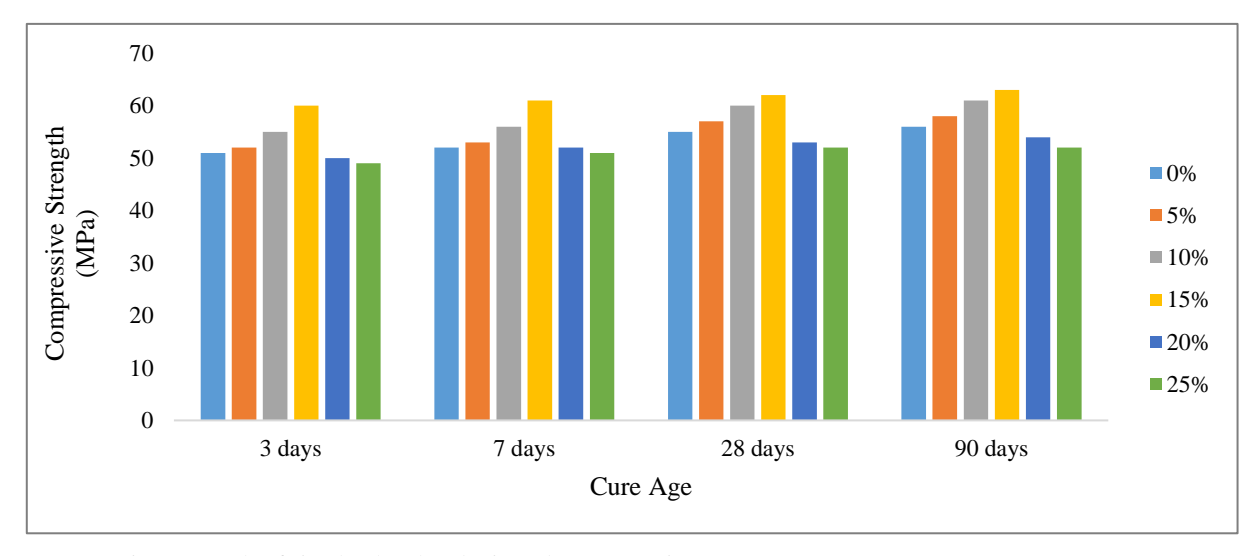


Figure 7. Compressive strength of rice husk ash substituted AAS specimens.

When analyzing the 3-day compressive strength data for Rice Husk Ash (RHA) blended concrete, it was observed that incorporating 5% RHA resulted in a 2% increase compared to the reference mix with 100% Ordinary Portland Cement (OPC). At 10% RHA, the increase rose to 7%, while 15% RHA achieved the highest gain at 17%. However, further increases in RHA content led to decreases in strength, with reductions of 2%, 4%, and 6% observed for 20%, 25%, and 30% RHA, respectively. Similarly, the 7-day strength data showed an optimal RHA content of 15%, which delivered an 18% improvement in strength compared to the reference. Lower proportions such as 5% and 10% RHA provided increases of 3% and 8%, respectively, while higher levels (20%, 25%, and 30%) exhibited diminishing returns, with the latter even showing a 3% reduction. These results consistently highlight that 15% RHA offers the best performance across both short and medium-term curing durations.

In line with these findings, long-term performance analysis over 90 days reaffirmed the superiority of the 15% RHA mix, maintaining the highest compressive strength over time. This underscores the potential of RHA to sustainably enhance the mechanical properties of concrete, particularly at an optimal replacement level of 15%. Supporting literature corroborates these outcomes. For instance, residual rice husk ash (RHA)

from Uruguay and RHA produced by controlled burning in the USA were compared for their effects on concrete properties, including compressive strength up to 91 days, splitting tensile strength, and air permeability, using cement replacement levels of 10% and 20% and water/cement ratios of 0.50, 0.40, and 0.32 (De Sensale, 2006). Similarly, partially replacing cement with rice husk ash (RHA) improves concrete's compressive strength, reduces water permeability, and enhances workability, with optimal results achieved at 10% replacement using ultra-fine RHA particles. However, finer RHA positively affects hardened concrete's properties but negatively impacts the workability of fresh concrete (Givi et al., 2010). Lastly, Huang et al. (2017) emphasized the ability of RHA to refine the pore structure and enhance both compressive strength and impermeability in high-performance concrete.

This comprehensive evaluation concludes that using 15% RHA in concrete mixtures is a highly effective strategy for improving compressive strength across varied curing durations, offering significant sustainability benefits and long-term performance advantages.

3.3. Flexural Strength

The flexural strength test results of AAS composite mortars are presented in Figure 8.

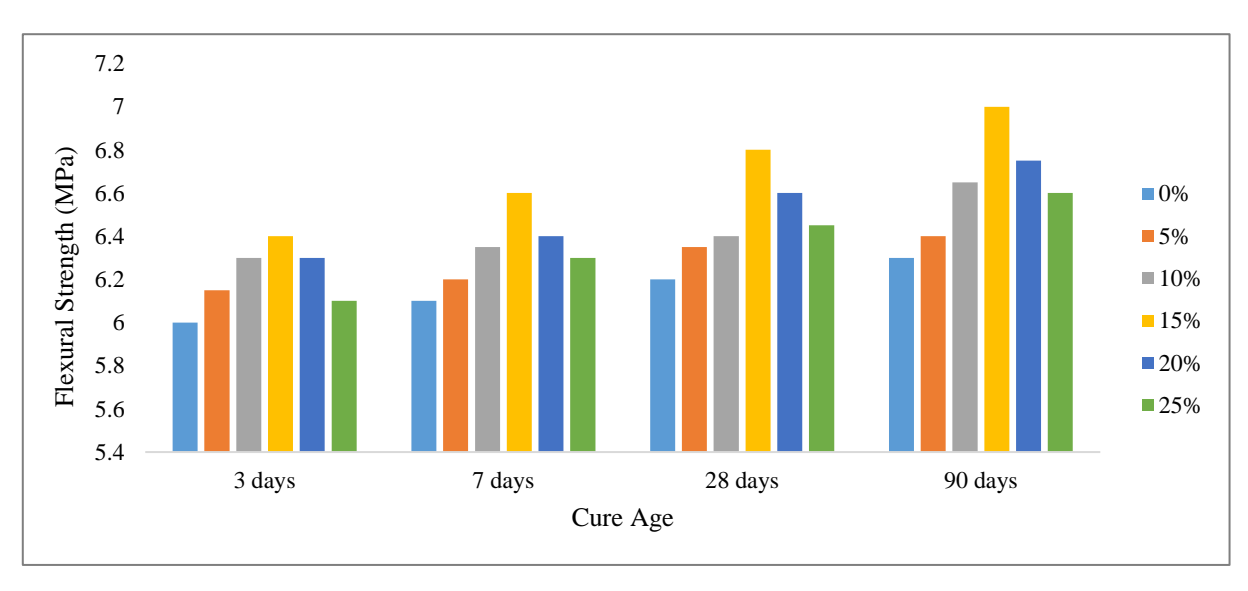


Figure 8. 7 and 28 day flexural strength results of AAS mortars.

The analysis of flexural strength for AAS mortars across curing periods of 3, 7, 28, and 90 days highlights the consistent performance of a 15% rice husk ash (RHA) mix. At 3 days, the 15% RHA mix achieved the highest strength (6.4 MPa), showcasing its short-term effectiveness. This trend continued over 7 and 28 days, with flexural strengths of 6.6 MPa and 6.8 MPa, respectively, affirming its medium- and long-term durability. By 90 days, the mix reached a peak flexural strength of 7.0 MPa, demonstrating sustained mechanical performance. These findings emphasize the efficiency of 15% RHA in

enhancing the mechanical properties of mortars. Supporting studies, such as Jamil et al. (2016), Ali et al. (2021), and Huang et al. (2017), confirm that RHA improves flexural strength by leveraging pozzolanic activity and refining pore structure. In conclusion, incorporating 15% RHA is a sustainable and optimal strategy for boosting the flexural performance of AAS mortars.

3.4. Compressive Strength of Glass Fiber-Reinforced AAS Composites

Figure 9 illustrates the effects of glass fiber reinforcement on the compressive strength of AAS composites. The study evaluated combinations of different glass fiber ratios (0%, 0.50%, 1%, 2%, 4%) and samples containing 0% and 15% rice husk ash (RHA) replacements.

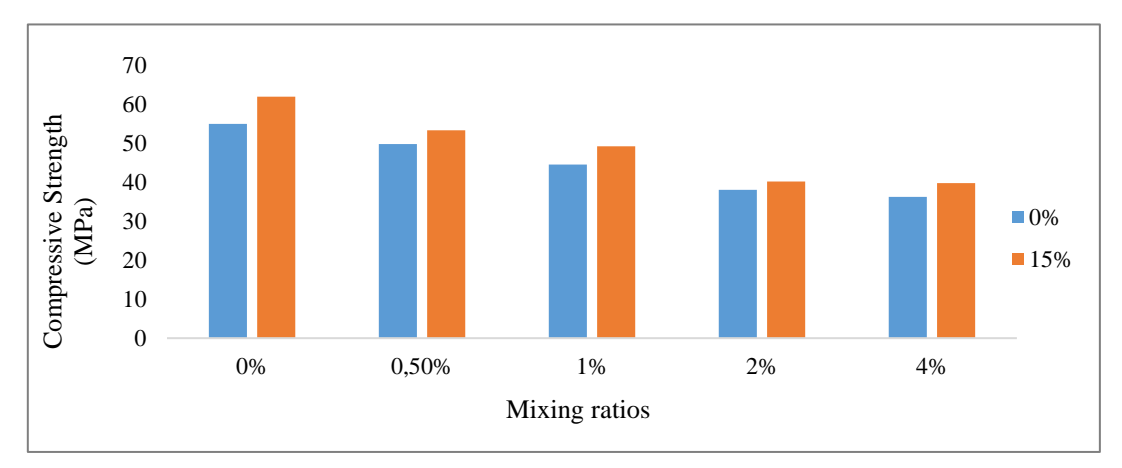


Figure 9. Compressive strength of glass fiber reinforced AAS samples.

The results indicate that increasing the glass fiber ratio generally improves compressive strength. For instance, in the absence of RHA (0%), higher glass fiber content significantly enhances compressive performance. Similarly, the inclusion of 15% RHA shows a synergistic effect with glass fibers, particularly at 2% fiber content, where the highest compressive strength was observed.

These findings align with existing research on fiber-reinforced composites. For example, Zheng et al. (2004) demonstrated that glass fiber reinforcement markedly improves compressive strength due to enhanced matrix-fiber interaction. Similarly, Kim and Crasto (1994) highlighted that unidirectional glass fiber composites exhibit superior compressive performance compared to random fiber arrangements.

In summary, the combination of glass fiber reinforcement and RHA optimizes the compressive strength of AAS

composites, with 2% glass fiber and 15% RHA providing the best results. This demonstrates the importance of tailoring fiber and matrix proportions for enhanced mechanical performance.

3.5. Flexural Strength of Glass Fiber-Reinforced AAS Composites

Figure 10 illustrates the changes in flexural strength of AAS composites with varying glass fiber ratios. The results show that increasing the glass fiber content generally enhances flexural strength, with the highest strength observed at 1% glass fiber. However, a decline in flexural strength was noted at 2%, suggesting that excessive glass fiber content may negatively impact performance. This highlights the importance of identifying an optimal glass fiber ratio to avoid overuse, which can compromise structural integrity.

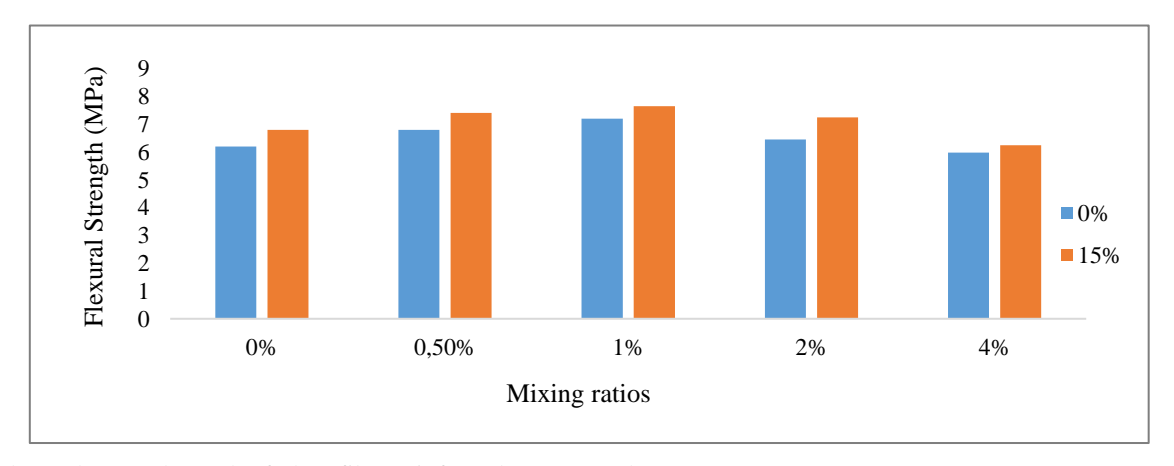


Figure 10. Flexural strength graph of glass fiber reinforced AAS samples.

Supporting studies align with these findings. Caixeta et al. (2015) demonstrated that incorporating glass fibers significantly improves the flexural strength of resin composites, emphasizing the reinforcement benefits provided by glass fibers. Similarly, Oberholzer et al. (2007) reported a 30% increase in flexural strength when glass fibers were added to composites, supporting the role of reinforcement in enhancing mechanical properties.

In conclusion, the addition of glass fibers positively impacts the flexural strength of AAS composites, with 1% being the optimal content. Proper calibration of fiber proportions is crucial for maximizing performance while preventing strength reductions due to overloading.

3.6. Water Absorption Variation

Figure 11 illustrates the water absorption change of AAS samples. The water absorption percentage of the samples increases relative to the "control sample" as the rice husk ash (RHA) content rises. This trend highlights the increasing impact of RHA on water absorption, which becomes more pronounced with higher RHA proportions. This behavior can be attributed to the unique properties of RHA, including its mineral composition, particle size, and reactivity, which influence water absorption characteristics.

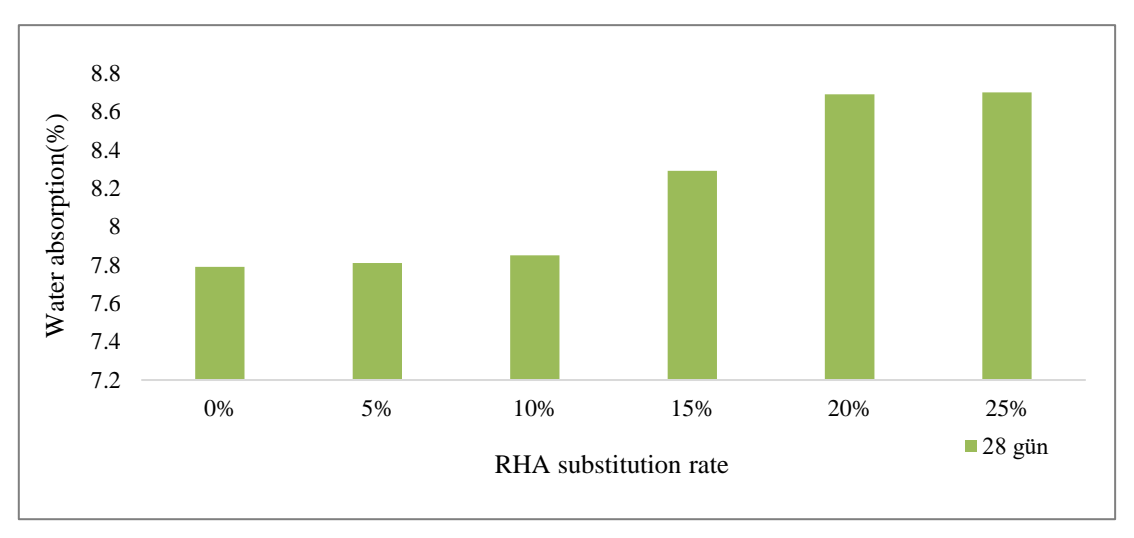


Figure 11. Water absorption change of AAS samples.

Supporting research confirms these observations. Huang et al. (2017) found that incorporating RHA into ultra-high-performance concrete reduced permeability due to the refined pore structure, enhancing impermeability at certain RHA levels. Similarly, Najigivi et al. (2012) demonstrated that ternary blends with RHA and nano-SiO₂ improved resistance to water absorption by forming a continuous, dense cement matrix, particularly at optimized replacement levels.

In summary, increasing RHA content significantly affects water absorption in concrete, with its mineral and structural characteristics playing a critical role. Optimizing the RHA content is essential to balancing enhanced durability with water absorption control.

3.7. Rapid Chloride Ion Permeability Test

The Rapid Chloride Ion Permeability Test (RCPT), conducted according to ASTM C1202 standards, is a critical

method for evaluating the chloride ion permeability and durability of construction materials. In this study, the effects of rice husk ash (RHA) content on the durability properties of alkali-activated cement (AAC) composites were investigated. Samples with RHA at 0%, 5%, 10%, 15%, 20%, 25%, and 30% were tested for chloride ion permeability at 28 and 90 days (Figure 12).

The 28-day results showed significant impacts of RHA on the permeability and resistance properties of AAC composites. Samples without RHA (0% RHA) exhibited high permeability and low resistance. Adding 5% RHA significantly reduced permeability and increased resistance. Samples with 10% RHA showed moderate permeability and resistance, while 15% RHA provided the lowest permeability and highest resistance values. Samples with 20% and 25% RHA displayed moderate permeability and resistance, while 30% RHA increased permeability and reduced resistance (Huang et al., 2017).

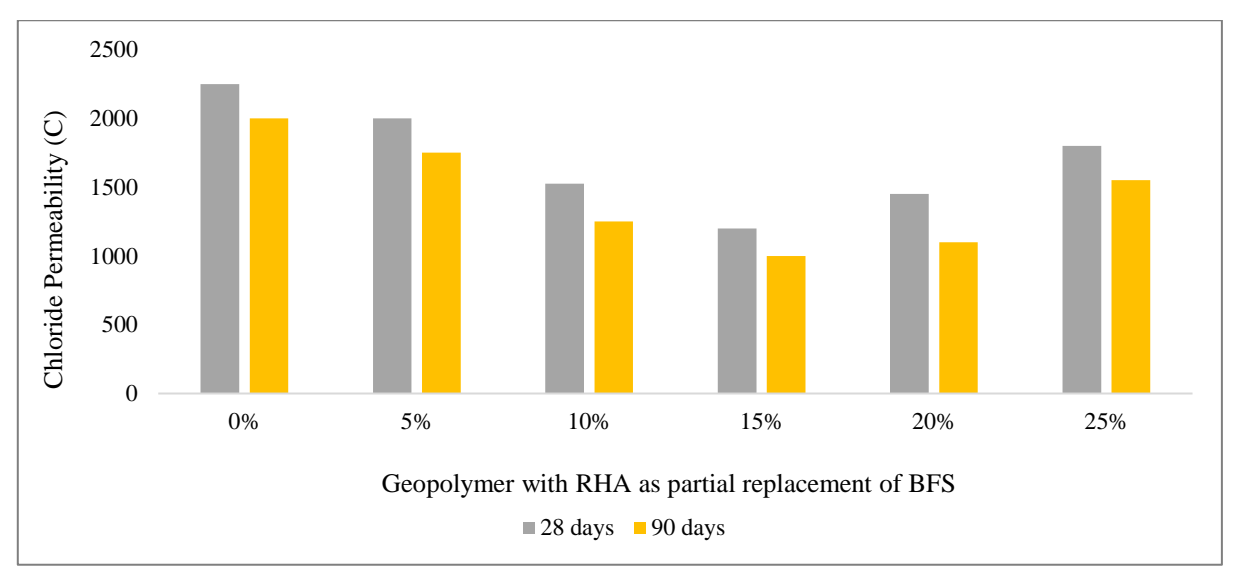


Figure 12. 28 and 90 day fast chloride ion permeability test results.

The 90-day results indicated that RHA reduces permeability and improves durability over time. AAC composites with 15% RHA achieved the lowest permeability and highest durability at 90 days, demonstrating excellent resistance to environmental effects (Prasittisopin & Trejo, 2017). As the water/cement ratio decreases in concrete, the reduction in chloride penetration is most effectively achieved with a 15% replacement of calcined rice husk ash (CRHA) or raw rice husk ash (RRHA) (De Sensale, 2010). Rice husk ash (RHA) has been shown to significantly enhance the durability and reduce the chloride ion permeability of AAC composites. De Sensale (2010) demonstrated that RHA, when used as a partial replacement for Portland cement, effectively improved the durability of cementitious materials by decreasing air permeability and chloride penetration, highlighting its suitability as a supplementary cementitious material. Similarly,

Ramezanianpour et al. (2018) found that nano RHA enhanced the long-term durability of mortars by improving chloride resistance, compressive strength, and electrical resistivity, confirming its role in improving concrete properties in aggressive environments. These studies collectively highlight the effectiveness of RHA in improving the performance and longevity of concrete structures. In conclusion, the incorporation of RHA, a sustainable agricultural byproduct, optimizes the durability and chloride resistance of AAC composites while contributing to environmentally friendly construction practices.

Figure 13 presents the compressive strength of alkaliactivated slag (AAS) composites under high-temperature effects.

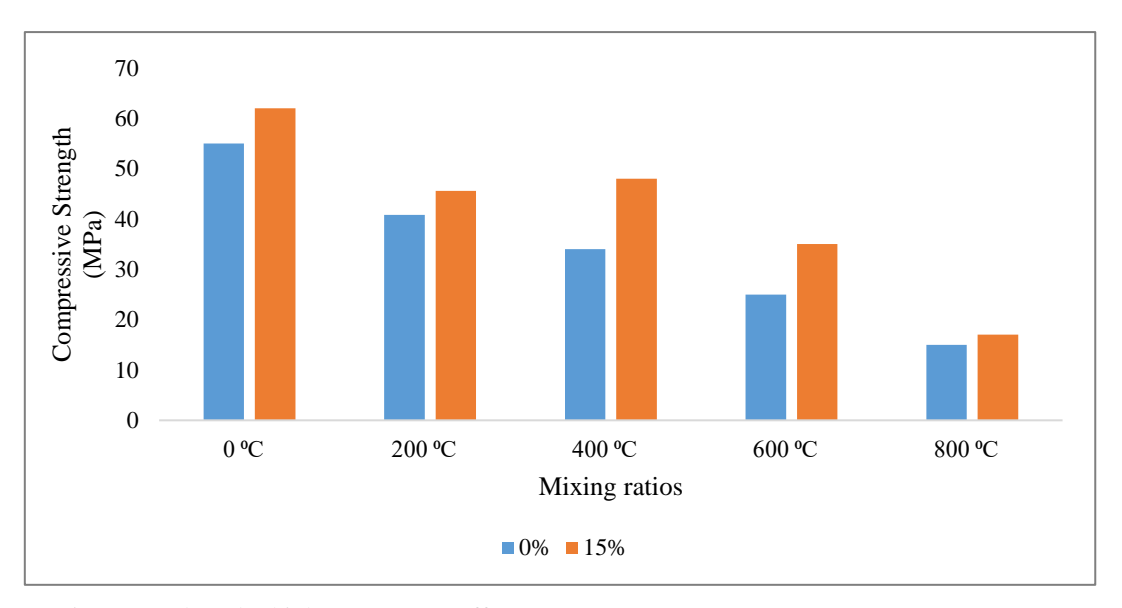


Figure 13. Compressive strength under high temperature effect.

The evaluation focuses on the effects of a 15% rice husk ash (RHA) addition on the 28-day compressive strength of the composites, subjected to varying temperature conditions of 200°C, 400°C, 600°C, and 800°C. The results indicated that RHA addition significantly enhanced compressive strength at 400°C and 600°C, demonstrating improved thermal resistance and mechanical performance. However, at 200°C and 800°C, the influence of RHA was more limited, with no significant differences observed at the higher temperature. Based on recent studies, Rice Husk Ash (RHA) is an effective alternative material for producing alkali-activated concrete (AAC), showing significant environmental benefits and durability. RHA, which is rich in silica, plays a key role in enhancing geopolymerization, improving mechanical properties such as compressive strength, and reducing permeability. Research indicates that when used in combination with other materials like fly ash or steel slag, RHA can significantly enhance concrete's ability to resist chemical attacks, such as from chloride or sulfuric acid exposure, making it highly suitable for harsh environments like marine settings Incorporating RHA into construction materials not only supports sustainable practices by reducing agricultural waste but also helps in addressing the growing demand for durable, high-performance concrete. Studies have shown that AAC made with RHA has comparable or even superior performance to traditional Portland Cement in terms of both durability and environmental impact (Alahmari et al., 2023; Barragán-Ramírez et al., 2024).

4. Conclusion

This study investigated the effects of sodium hydroxide molarity, curing temperature, rice husk ash (RHA) addition, and glass fiber reinforcement on the mechanical properties and durability of alkali-activated slag (AAS) composites. The findings demonstrate that increasing the molarity of sodium hydroxide solutions enhances compressive strength, with the most effective conditions observed at 12M molarity and 110°C curing temperature. These parameters promoted optimal geopolymerization, resulting in superior mechanical performance.

The incorporation of RHA significantly improved the flexural strength of AAS composites, with the highest strength achieved at a 15% RHA addition. This optimal mix also maintained its high strength over long-term use while effectively reducing chloride ion permeability, highlighting its suitability for applications requiring enhanced durability. Furthermore, under elevated temperatures, particularly at 400°C and 600°C, the addition of RHA further increased compressive strength, underscoring its thermal stability benefits.

Glass fiber reinforcement also contributed positively to both flexural and compressive strength. However, a decline in performance was observed at 2% glass fiber content, emphasizing the necessity of carefully selecting the optimal fiber dosage for maximizing mechanical benefits.

In summary, the synergistic effects of RHA and glass fiber additions were found to be effective strategies for enhancing the mechanical properties and durability of AAS composites. These findings underline the potential of incorporating RHA and glass fibers in concrete designs to improve environmental sustainability and long-term structural performance, offering valuable insights for future construction material innovations.

Acknowledgment

This research was supported under the scope of the Scientific and Technological Research Council of Turkey (TÜBİTAK) 2209-A University Students Research Projects Support Program, 2nd term of 2022, with project number 1919B012213936.

Conflict of Interest

The authors declare that they have no conflict of interest.

References

- Adam, A. A., & Horianto, X. X. X. (2014). The effect of temperature and duration of curing on the strength of fly ash based geopolymer mortar. *Procedia Engineering*, 95, 410-414. https://doi.org/10.1016/j.proeng.2014.12.199
- Alahmari, T. S., Abdalla, T. A., & Rihan, M. A. M. (2023). Review of recent developments regarding the durability performance of eco-friendly geopolymer concrete. *Buildings*, *13*(12), 3033. https://doi.org/10.3390/buildings13123033
- Ali, T., Saand, A., Bangwar, D. K., Buller, A. S., & Ahmed, Z. (2021). Mechanical and durability properties of aerated concrete incorporating rice husk ash (RHA) as partial replacement of cement. *Crystals*, 11(6), 604. https://doi.org/10.3390/cryst11060604
- Amran, M., Al-Fakih, A., Chu, S. H., Fediuk, R., Haruna, S., Azevedo, A., & Vatin, N. (2021). Long-term durability properties of geopolymer concrete: An in-depth review. *Case Studies in Construction Materials*, *15*, e00661. https://doi.org/10.1016/J.CSCM.2021.E00661
- Arularasi, V., Thamilselvi, P., Avudaiappan, S., Saavedra Flores, E. I., Amran, M., Fediuk, R., Vatin, N., & Karelina, M. (2021). Rheological behavior and strength characteristics of cement paste and mortar with fly ash and GGBS admixtures. *Sustainability*, *13*(17), 9600. https://doi.org/10.3390/su13179600
- ASTM International. (2002). ASTM C109/C109M-02: Standard test method for compressive strength of

- hydraulic cement mortars (using 2-in. or [50-mm] cube specimens). https://cdn.standards.iteh.ai/samples/18736/1886184914c84503a7c2e10762f27381/ASTM-C109-C109M-02.pdf
- ASTM International. (2003). *ASTM C597-16: Standard test method for pulse velocity through concrete*. https://cdn.standards.iteh.ai/samples/94392/666ac7ceb8 354eefaab00c9ca74b2b1f/ASTM-C597-16.pdf
- ASTM International. (2006). ASTM C642-06: Standard test method for density, absorption, and voids in hardened concrete.
 - $\frac{https://cdn.standards.iteh.ai/samples/48531/2dda55d49}{db741ebad1d409bacd4f0f8/ASTM-C642-06.pdf}$
- ASTM International. (2012). ASTM C1202: Standard test method for electrical indication of concrete's ability to resist chloride ion penetration. https://cdn.standards.iteh.ai/samples/79981/7d0c052c7f4c4e9f9d037138c568a532/ASTM-C1202-12.pdf
- Barragán-Ramírez, R., González-Hernández, A., Bautista-Ruiz, J., Ospina, M., & Aperador Chaparro, W. (2024). Enhancing concrete durability and strength with fly ash, steel slag, and rice husk ash for marine environments. *Materials*, *17*(12), 3001. https://doi.org/10.3390/ma17123001
- Caixeta, R. V., Guiraldo, R. D., Berger, S. B., Kaneshima, E. N., Júnior, É. M. F., Drumond, A. C., Júnior, A. G., & Lopes, M. B. (2015). Influence of glass-fiber reinforcement on the flexural strength of different resin composites. *Applied Adhesion Science*, *3*, 24. https://doi.org/10.1186/s40563-015-0053-1
- Colangelo, F., Farina, I., Travaglioni, M., Salzano, C., Cioffi, R., & Petrillo, A. (2021). Eco-efficient industrial waste recycling for the manufacturing of fibre reinforced innovative geopolymer mortars: Integrated waste management and green product development through LCA. *Journal of Cleaner Production*, 312, 127777. https://doi.org/10.1016/J.JCLEPRO.2021.127777
- De Sensale, G. R. (2006). Strength development of concrete with rice-husk ash. *Cement and Concrete Composites*, 28(2), 158-160. https://doi.org/10.1016/j.cemconcomp.2005.09.005
- De Sensale, G. R. (2010). Effect of rice-husk ash on durability of cementitious materials. *Cement and Concrete Composites*, 32(9), 718-725. https://doi.org/10.1016/j.cemconcomp.2010.07.008
- Givi, A. N., Rashid, S. A., Aziz, F. N. A., & Salleh, M. A. M. (2010). Assessment of the effects of rice husk ash particle size on strength, water permeability and

- workability of binary blended concrete. *Construction and Building Materials*, 24(11), 2145-2150. https://doi.org/10.1016/j.conbuildmat.2010.04.045
- Habert, G., D'Espino De Lacaillerie, J. B., & Roussel, N. (2011). An environmental evaluation of geopolymer-based concrete production: Reviewing current research trends. *Journal of Cleaner Production*, 19(11), 1229-1238. https://doi.org/10.1016/J.JCLEPRO.2011.03.012
- Hardjito, D., & Rangan, B. V. (2005). Development and properties of low-calcium fly ash-based geopolymer concrete.

 https://espace.curtin.edu.au/bitstream/handle/20.500.11
 - https://espace.curtin.edu.au/bitstream/handle/20.500.11 937/5594/19327 downloaded stream 419.pdf?sequen ce=2
- Hossain, S. S., Roy, P. K., & Bae, C. J. (2021). Utilization of waste rice husk ash for sustainable geopolymer: A review. *Construction and Building Materials*, 310, 125218.
 - https://doi.org/10.1016/J.CONBUILDMAT.2021.1252 18
- Huang, H., Gao, X., Wang, H., & Ye, H. (2017). Influence of rice husk ash on strength and permeability of ultra-high performance concrete. *Construction and Building Materials*, 149, 621-628. https://doi.org/10.1016/j.conbuildmat.2017.05.155
- Hwang, C. L., & Huynh, T. P. (2015). Effect of alkali-activator and rice husk ash content on strength development of fly ash and residual rice husk ash-based geopolymers. *Construction and Building Materials*, 101(Part 1), 1-9. https://doi.org/10.1016/J.CONBUILDMAT.2015.10.02
- Jamil, M., Khan, M. N. N., Karim, M. R., Kaish, A. B. M. A., & Zain, M. F. M. (2016). Physical and chemical contributions of Rice Husk Ash on the properties of mortar. *Construction and Building Materials*, 128, 185-198. https://doi.org/10.1016/j.conbuildmat.2016.10.029
- Kim, R. Y., & Crasto, A. S. (1994). Longitudinal compression strength of glass fiber-reinforced composites. *Journal of Reinforced Plastics and Composites*, *13*(4), 326-338. https://doi.org/10.1177/073168449401300404
- Kim, Y. Y., Lee, B. J., Saraswathy, V., & Kwon, S. J. (2014).
 Strength and durability performance of alkali-activated rice husk ash geopolymer mortar. *Scientific World Journal*, 2014(1), 209584.
 https://doi.org/10.1155/2014/209584
- Manzoor, T., Bhat, J. A., & Shah, A. H. (2024). Performance of geopolymer concrete at elevated temperature— A critical review. *Construction and Building*

- *Materials*, *420*, 135578. https://doi.org/10.1016/j.conbuildmat.2024.135578
- Mathew, G., & Issac, B. M. (2020). Effect of molarity of sodium hydroxide on the aluminosilicate content in laterite aggregate of laterised geopolymer concrete. *Journal of Building Engineering*, *32*, 101486. https://doi.org/10.1016/j.jobe.2020.101486
- Mathew, G., & Joseph, B. (2018). Flexural behaviour of geopolymer concrete beams exposed to elevated temperatures. *Journal of Building Engineering*, *15*, 311-317. https://doi.org/10.1016/J.JOBE.2017.09.009
- Mehta, A., & Siddique, R. (2018). Sustainable geopolymer concrete using ground granulated blast furnace slag and rice husk ash: Strength and permeability properties. *Journal of Cleaner Production*, 205, 49-57. https://doi.org/10.1016/J.JCLEPRO.2018.08.313
- Memon, F. A., Nuruddin, M. F., Khan, S., Shafiq, N., & Ayub, T. (2013). Effect of sodium hydroxide concentration on fresh properties and compressive strength of self-compacting geopolymer concrete. *Journal of Engineering Science and Technology*, 8(1), 44-56.
- Najigivi, A., Abdul Rashid, S., Nora A. Aziz, F., & Mohd Salleh, M. A. (2012). Water absorption control of ternary blended concrete with nano-SiO 2 in presence of rice husk ash. *Materials and Structures*, *45*, 1007-1017. https://doi.org/10.1617/s11527-011-9813-y
- Oberholzer, T. G., Du Preez, I. C., Lombard, R., & Pitout, E. (2007). Effect of woven glass fibre reinforcement on the flexural strength of composites: Scientific. *South African Dental Journal*, 62(9), 386-389.
- Prasittisopin, L., & Trejo, D. (2017). Performance characteristics of blended cementitious systems

- incorporating chemically transformed rice husk Ash. *Advances in Civil Engineering Materials*, *6*(1), 17-35. https://doi.org/10.1520/ACEM20160001
- Ramezanianpour, A., Balapour, M., & Hajibandeh, E. (2018).

 Effect of nano rice husk ash against penetration of chloride ions in mortars. *AUT Journal of Civil Engineering*, 2(1), 97-102.

 https://doi.org/10.22060/ajce.2017.12387.5203
- Sarker, P. K., Haque, R., & Ramgolam, K. V. (2013). Fracture behaviour of heat cured fly ash based geopolymer concrete. *Materials* & *Design*, 44, 580-586. https://doi.org/10.1016/j.matdes.2012.08.005
- Singh, N. B., & Middendorf, B. (2020). Geopolymers as an alternative to Portland cement: An overview. *Construction and Building Materials*, 237, 117455.
 - https://doi.org/10.1016/j.conbuildmat.2019.117455
- Sturm, P., Gluth, G. J. G., Brouwers, H. J. H., & Kühne, H. C. (2016). Synthesizing one-part geopolymers from rice husk ash. *Construction and Building Materials*, 124, 961-966.
 - https://doi.org/10.1016/j.conbuildmat.2016.08.017
- Zhan, J., Liu, W., Wu, F., Li, Z., & Wang, C. (2018). Life cycle energy consumption and greenhouse gas emissions of urban residential buildings in Guangzhou city. *Journal of Cleaner Production*, 194, 318-326. https://doi.org/10.1016/j.jclepro.2018.05.124
- Zheng, Y., Ning, R., & Zheng, Y. (2004). Glass fiber-reinforced polymer composites of high compressive strength. *Journal of Reinforced Plastics and Composites*, 23(16), 1729-1740. https://doi.org/10.1177/0731684404040127